

Nanostructured Hybrid Materials Formed by Cell Reaction between Polycarbazole and Metals

Tomochika Miyazaki, Sang-Kook Kim, and Katsuyoshi Hoshino*

Faculty of Engineering, Chiba University, 1-33 Yayoi-cho, Inage-ku, Chiba 263-8522, Japan

Received March 14, 2006. Revised Manuscript Received August 28, 2006

Aluminum films are vacuum-evaporated onto a ClO_4^- -doped green polycarbazole (PCz) film. The appearance of the resulting aluminum/PCz junctions drastically changes with time; the time-dependent fading of the metallic white color and green color of the PCz is observed during their storage in air, and colorless films are obtained several hours after the evaporation. Various microscopic analyses of the resultant films revealed that they consist of an undoped PCz film with a nanosized region of aluminum compounds being dispersed in it. Vibrational spectroscopy of the films before and after the hybridization shows the chemical interaction between the aluminum compounds and the carbazole ring. The electric conductivity, work function, and UV–vis absorption of the hybrid films are measured as a function of the amount of evaporated aluminum. The alternate use of indium is also reported.

1. Introduction

The interfaces of conducting polymer/inorganic semiconductors and conducting polymer/metals have attracted much attention over the last few decades.¹ The electronic (or chemical) interactions at the former interface determine the performance of the junction devices; the more intimate the interaction, the better the junction characteristics.² The latter interface also contributes to the junction formation and characteristics;³ however, more interestingly, a solid-state reaction occurs at the interface⁴ depending on the combination of the conducting polymer and metal, and a novel organic–inorganic hybrid material is spontaneously formed.^{4c} Our recent study revealed that the electropolymerized polypyrrole (PPy) film reacts with an evaporated aluminum layer under an ambient atmosphere to produce a PPy–aluminum oxide/hydroxide hybrid film and that the durability of the

hybrid film against redox cyclings is significantly improved compared with the nonmodified PPy film.^{4c} A preliminary study suggested that the hybridization is induced by the cell reaction between the anion-doped PPy film (electron-deficient high-work-function material) and the low-work-function metals (Al and In). This reaction would be initiated by electron transfer from the metal to the PPy, followed by the conversion of the metals to the corresponding oxide/hydroxide (and/or salts) and the dedoping of the PPy film.

On the other hand, electropolymerized polycarbazole (PCz) films are expected to be candidates for electroluminescent,⁵ electrochromic,⁶ and photoconductive materials,⁷ though they are much less studied compared to polypyrrole, polythiophene, polyaniline, and their derivatives. The intriguing properties of the PCz films are their highest doping levels^{6a,8} of 45–50% among the conducting polymers studied so far (doping level is defined as the number of anions per one monomer unit) and their color change from nearly transparent white (undoped state) to green (doped state).⁹ The former property would be preferred for the hybridization reaction described above since the more abundant reaction species

* Corresponding author. E-mail: k_hoshino@faculty.chiba-u.jp.

- (1) (a) Burkstrand, J. M. *J. Appl. Phys.* **1981**, *52*, 4795–4800. (b) Kanicki, J. Polymeric Semiconductor Contacts and Photovoltaic Applications. In *Handbook of Conducting Polymers*; Scotheim, T. A., Ed.; Marcel Dekker: New York, 1986; Vol. 1. (c) Fahlman, M.; Salaneck, W. R. *Surf. Sci.* **2002**, *500*, 904–922.
- (2) (a) Hoshino, K.; Ogata, T.; Kokado, H. *Jpn. J. Appl. Phys., Part 2* **1995**, *34*, L1421–L1423. (b) Hoshino, K.; Tokutomi, K.; Iwata, Y.; Kokado, H. *J. Electrochem. Soc.* **1998**, *145*, 711–720. (c) Hoshino, K.; Inui, M.; Kitamura, T.; Kokado, H. *Electrochem. Solid-State Lett.* **2000**, *3*, 426–428. (d) Ogawa, T.; Takase, S.; Kitamura, T.; Hoshino, K. *Hyomen Kagaku* **2004**, *25*, 392–400.
- (3) (a) Grant, P. M.; Tani, T.; Gill, W. D.; Krounbi, M.; Clarke, T. C. *J. Appl. Phys.* **1981**, *52*, 869–872. (b) Inganäs, O.; Skotheim, T.; Lundström, I. *J. Appl. Phys.* **1983**, *54*, 3636–3639. (c) Kaneto, K.; Takashima, W. *Curr. Appl. Phys.* **2001**, *1*, 355–361. (d) Saxena, V.; Santhanam, K. S. V. *Curr. Appl. Phys.* **2003**, *3*, 227–233. (e) Chung, S.-F.; Wen, T.-C.; Gopalan, A. *Mater. Sci. Eng. B* **2005**, *116*, 125–130.
- (4) (a) Uehara, K.; Ichikawa, T.; Serikawa, T.; Yoshikawa, S.; Ehara, S.; Tsunooka, M. *Thin Solid Films* **1998**, *322*, 198–205. (b) De Souza, S.; Pereira Da Silva, J. E.; Córdoba de Torresi, S. I.; Temperini, M. L. A.; Torresi, R. M. *Electrochem. Solid-State Lett.* **2001**, *4*, B27–B30. (c) Watanabe, H.; Kitamura, T.; Hoshino, K. *Electrochem. Solid-State Lett.* **2003**, *6*, D1–D4. (d) José, E.; Pereira da Silva, J. E.; Córdoba de Torresi, S. I.; Torresi, R. M. *Corros. Sci.* **2005**, *47*, 811–822. (e) Torresi, R. M.; De Souza, S.; Pereira Da Silva, J. E.; Córdoba de Torresi, S. I. *Electrochim. Acta* **2005**, *50*, 2213–2218.

- (5) (a) Abe, S. Y.; Bernede, J. C.; Delvalle, M. A.; Tregouet, Y.; Ragot, F.; Diaz, F. R.; Lefrant, S. *Synth. Met.* **2002**, *126*, 1–6. (b) Baba, A.; Onishi, K.; Knoll, W.; Advincula, R. C. *J. Phys. Chem. B* **2004**, *108*, 18949–18955.
- (6) (a) Mengoli, G.; Musiani, M. M.; Schreck, B.; Zecchin, S. *J. Electroanal. Chem.* **1988**, *246*, 73–86. (b) Chevrot, C.; Ngbilu, E.; Kham, K.; Sadki, S. *Synth. Met.* **1996**, *81*, 201–204. (c) Verghese, M. M.; Ram, M. K.; Vardhan, H.; Malhotra, B. D.; Ashraf, S. M. *Polymer* **1997**, *38*, 1625–1629. (d) Tran-Van, F.; Henri, T.; Chevrot, C. *Electrochim. Acta* **2002**, *47*, 2927–2936.
- (7) (a) Gill, W. D. *J. Appl. Phys.* **1972**, *43*, 5033–5040. (b) Reucroft, P. J.; Ghosh, S. K. *Phys. Rev. B* **1973**, *8*, 803–807. (c) Gražulevičius, J. V.; Kubickas, R.; Undėenas, A. *Eur. Polym. J.* **1992**, *28*, 539–545. (d) Huang, J.; Xu, Y.; Hou, Q.; Yang, W.; Yuan, M.; Cao, Y. *Macromol. Rapid Commun.* **2002**, *23*, 709–712. (e) Morin, J. F.; Leclerc, M.; Adès, D.; Siove, A. *Macromol. Rapid Commun.* **2005**, *26*, 761–778.
- (8) Bargon, J.; Mohmand, S.; Waltman, R. J. *IBM J. Res. Develop.* **1983**, *27*, 330–341.
- (9) Tran-Van, F.; Henri, T.; Chevrot, C. *Electrochim. Acta* **2002**, *47*, 2927–2936.

in the polymer film (cation radicals and dications which pair with dopant anions) allow for the reaction with a larger amount of metals. The nearly colorless feature in the undoped state is important in the field of imaging science and technology (e.g., organic electroluminescent and electrochromic materials). These unique properties drove us to use the PCz film for the formation of hybrid films.

In this study, it is shown that hybridization occurs between the PCz film and metals (Al and In) and that the resultant hybrid film has a unique nanostructure with the metal compounds being dispersed in a PCz backbone. Additionally, the hybridization is accompanied by a drastic color change from green to nearly colorless, which helps to understand the mechanism of the hybridization reaction (the color change for the PPy film was not clearly visible to the naked eye because it is intensely colored in both the doped and undoped states).^{4c}

2. Experimental Section

The PCz films were prepared on an indium-tin-oxide coated glass plate (ITO, Geomatech, 10 Ω /sq) by the electro-oxidation of 5 mM carbazole (Tokyo Kasei Kogyo, 98%) dissolved in a dichloromethane solution containing tetrabutylammonium perchlorate (TBAP, 0.1 M) or tetraethylammonium perchlorate (TEAP, 0.065 M) at 20 °C under an N₂ atmosphere. The working ITO and the counter Pt plates were immersed in the main compartment of the electrolysis cell. In the auxiliary compartment, which is separated from the main one by a sintered glass frit, was immersed a KCl agar bridge connected to the reference saturated calomel electrode (SCE). Prior to the electrolysis, the ITO and Pt plates were ultrasonically washed in distilled–deionized water and then in acetone each 10 min. The resultant PCz films were washed with dichloromethane and dried in air, and then the metal layers were evaporated on the PCz films. During the evaporation, a glass plate was placed adjacent to the PCz/ITO sample. The thicknesses of the metal layer on the glass plate were determined by atomic force microscopic measurements (SEIKO instrument, model Nanopics 1000) and were regarded as being equal to those evaporated on the PCz films. The morphology of the hybrid films was investigated by transmission electron microscopic (TEM, Hitachi FE-TEM HF-2200) and scanning electron microscopic (SEM, Topcon ABT-32) observations. X-ray photoelectron spectroscopy (XPS, ULVAC phi ESCA 5400 spectrometer with Al K α radiation, the binding energy scale was obtained by setting the C 1s peak to 284.6 eV) and energy-dispersive X-ray analysis (EDX, Noran Vantage EDS system) were employed for the compositional analyses of the sample films. The electric conductivity (σ) and work function (ϕ) of the sample films were determined in air (ca. 20 °C, 40% RH) by a four-point probe method (Mitsubishi Chemical Loresta-GP MCP-T600 equipped with a PSP probe) and a contact-potential difference (CPD) measurement (Trek 320B electrostatic voltmeter),¹⁰ respectively. The CPD values for the samples were referenced to a vacuum-evaporated Au film. Fourier transform infrared (FT-IR) spectra were recorded using a JASCO 410 FT-IR spectrometer.

3. Results and Discussion

3.1. Electropolymerization Behavior of Carbazole.

Curve a in Figure 1 shows the linear sweep voltammogram

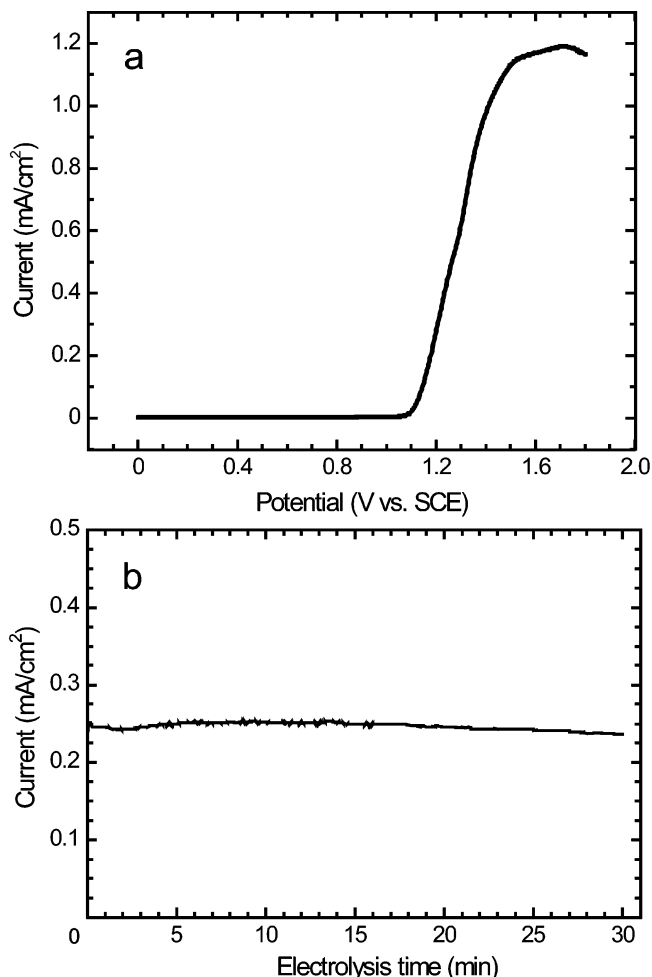


Figure 1. Oxidation behavior of carbazole. Part a shows the linear sweep voltammogram of carbazole (5 mM) in a TBAP(0.1 M)/dichloromethane system at an ITO electrode ($1.5 \times 1.5 \text{ cm}^2$) under an N₂ atmosphere: Sweep rate, 20 mV/s; temperature, 10 °C. Part b is the current–time curve during the controlled-potential electropolymerization of carbazole at 1.2 V vs SCE in the TBAP(0.1 M)/dichloromethane system at 10 °C under an N₂ atmosphere.

of carbazole (5 mM) in a dichloromethane solution containing 0.1 M TBAP at 10 °C under an N₂ atmosphere. The oxidation current steeply rose at 1.1 V and was accompanied by the deposition of a bluish-green film. Based on this voltammogram, films were deposited by the controlled-potential electrolysis at 1.2, 1.3, 1.4, and 1.6 V. The film prepared at 1.6 V was brittle and partially peeled off from the ITO when washed in dichloromethane. Ambrose and Nelson¹¹ measured the cyclic voltammogram of carbazole (2 mM) in an acetonitrile solution containing 0.1 M TEAP at a Pt electrode and observed an oxidation peak current at 1.2 V vs SCE. Their chronoamperometric and chronopotentiometric measurements suggested that the oxidation wave is assigned to the formation of the carbazole cation radical, the coupling of the cation radical with another cation radical or with a parent molecule to form 3,3'-dicarbazyl (major) and 9,9'-dicarbazyl (small amounts), further oxidation of 3,3'-dicarbazyl to the quinoidal dication, and the follow-up reaction of 3,3'-dicarbazyl with carbazole. They also observed an oxidation wave at 1.8 V (peak potential) and

(10) Veregin, R. P. N.; Powell, D.; Tripp, C. P.; McDougall, M. N. V.; Mahon, M. J. *Imaging Sci. Technol.* **1997**, *41*, 192–196.

(11) Ambrose, J. F.; Nelson, R. F. *J. Electrochem. Soc.* **1968**, *115*, 1159–1164.

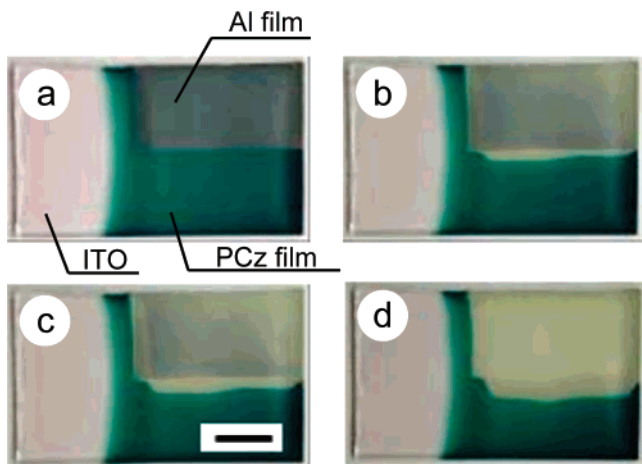


Figure 2. Photographs showing the reaction of PCz with evaporated Al. Fading of metallic color with time, t , is clearly demonstrated in the images taken at $t = 2$ min (a), 1 h (b), 1.5 h (c), and 6 h (d) under ambient conditions. Scale bar: 5 mm.

assigned it to the oxidation of 9,9'-dicarbazyl to the unknown products. Mengoli et al.^{6a} recorded the cyclic voltammogram of carbazole (5 mM) in the mixture of 75 vol % CH₃OH and 25% HClO₄ aqueous solution (5 M) at an Au electrode and found that resistive films were formed when the upper oxidation limit is higher than 1.00 V. Based on these data, our film prepared at 1.6 V would involve unknown resistive products and, therefore, is not adequate for our objective, so films were hereinafter prepared at 1.2 V (although the applied potentials of 1.3 and 1.4 V also led to coherent filming, the potential of 1.2 V was preferred as the resulting films showed better homogeneity). The plot of the film thickness versus the amount of electricity per unit area of the ITO (Q) gave the deposition rate of 16 nm/mC cm⁻². The equivalent deposition rate was obtained by the electropolymerization of carbazole (5 mM) in a dichloromethane/TEAP(0.065 M) system at 1.4 V. Curve b in Figure 1 shows the current density–time transient recorded when the ITO was stepped from 0.0 to 1.2 V. A steady current of 0.25 mA/cm² was obtained as occurs for the nucleation of a noninsulating film.

3.2. Solid-State Reaction of PCz Film with Aluminum Metal. The PCz/Al system exhibited a color change with storage time, t , in air (20 °C, ca. 50% RH) as shown in Figure 2; $t = 0$ corresponds to the time at which air is introduced into the vacuum chamber used for the evaporation of Al. The Al layer was evaporated on the upper half of the green PCz film. At $t = 2$ min, the Al layer exhibited a metallic white color (photograph a); however, the color faded with time as demonstrated by photographs b ($t = 1$ h), c ($t = 1.5$ h), and d ($t = 6$ h). In response to this fading of Al, the green color of the PCz film was bleached and the colorless film was obtained. Figure 3 shows the UV–vis absorption spectra for the color change demonstrated in Figure 2 (spectra a–d). The spectrum of the PCz film with no evaporated Al layer (spectrum e) has signals at ca. 400 and 670 nm due to the dicarbazyl cation radical.¹² Upon contacting of the PCz film with the Al layer, the absorption bands at 400 and 670 nm abruptly disappeared at $t = 2$ min, and the resulting structureless absorption gradually decreased with t and finally

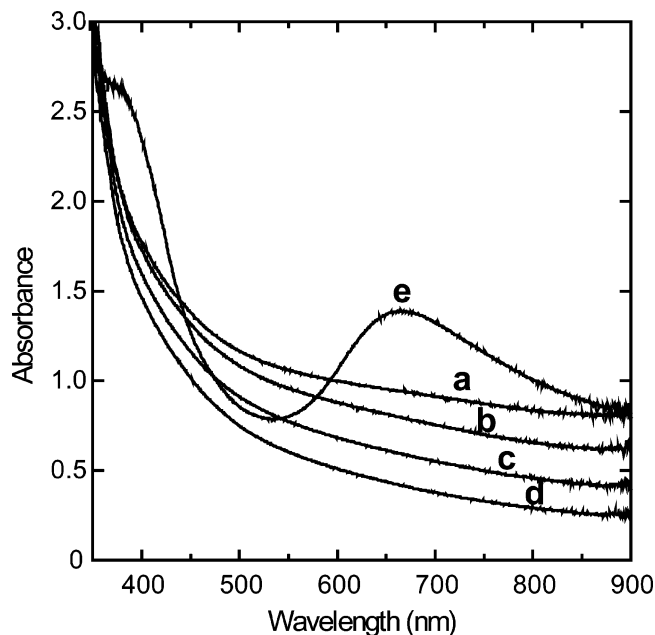


Figure 3. Change in the UV–vis absorption spectrum of the PCz film with t : $t = 2$ min (a), 1 h (b), 2 h (c), and 24 h (d) under ambient conditions. Curve (e) is the spectrum of the PCz single film.

reached a steady value at $t = 24$ h. This spectral change in shape is quite similar to the electrochemical dedoping behavior of the PCz derivative film,¹³ suggesting that the dedoping occurs during the solid-state reaction between the PCz film and the Al layer. When the Al(18 nm)-deposited PCz film ($Q = 70$ mC cm⁻²) was stored in a vacuum (10⁻³ Pa), no change in the Al layer was observed even after its storage for 3 days. However, the reaction shown in Figure 2 occurred when the vacuum was broken. Additionally, the reaction was accelerated by placing drops of water on the Al layer. No reaction was induced by the alternate use of an Au layer instead of the Al layer. The Al layer evaporated on a glass plate and the PCz film formed on the ITO were unchanged by their storage in air for at least a few years. All these observations and results for the PCz/Al film are the same as those for the previously reported polypyrrole/Al film,^{4c} and according to the report, the reaction demonstrated by Figures 2 and 3 may be explained on the basis of the following galvanic corrosion and dedoping reactions:^{4c} Upon Al deposition, the junction with a large work-function (ϕ) difference is formed between the Al film ($\phi = 4.3$ eV)¹⁴ and the as-grown PCz film ($\phi = 5.5$ eV, see section 3.5). Under ordinary pressure and temperature (20 °C and 40% RH conditions), adsorbed water¹⁵ should cover the junction and intervene between the two films at the sites with structural defects, such as microcracks, microscratches, and pinholes. At such sites, the electropositive PCz film may give rise to a local corrosion cell with the electronegative

- (12) (a) Ambrose, J. F.; Carpenter, L. L.; Nelson, R. F. *J. Electrochem. Soc.* **1975**, *122*, 876–894. (b) Kessel, R.; Schultze, J. W. *Surf. Interface Anal.* **1990**, *16*, 401–406. (c) Verghese, M. M.; Basu, T.; Malhotra, B. D. *Mater. Sci. Eng.* **1995**, *C3*, 215–218.
- (13) Chevrot, C.; Ngbilo, E.; Kham, K.; Sadki, S. *Synth. Met.* **1996**, *81*, 201–204.
- (14) Michaelson, H. B. *J. Appl. Phys.* **1977**, *48*, 4729–4733.
- (15) (a) Liu, Y.-C.; Hwang, B.-J. *J. Electroanal. Chem.* **2001**, *501*, 100–106. (b) González, J. A.; Morcillo, M.; Escudero, E.; López, V.; Otero, E. *Surf. Coat. Technol.* **2002**, *153*, 225–234.

aluminum film, and electron transfer from the latter to the former film occurs which is driven by the difference in their work functions. The anodic oxidation of Al to Al^{3+} is followed by its conversion to the corresponding oxide/hydroxide ($\text{Al}_2\text{O}_3 \cdot 3\text{H}_2\text{O}$ or $\text{Al}(\text{OH})_3$)^{15b,16} and the perchlorate salt ($\text{Al}(\text{ClO}_4)_3$, see below). The cathodic reactions may involve the reduction of the cationic species (polaron and bipolaron) and the reduction of protons that form along with aluminum oxide/hydroxide during the corrosion reaction in natural environments.^{15b,16} The former reduction causes release of ClO_4^- from the PCz backbone (dedoping) and the resultant ClO_4^- is coupled with the Al^{3+} to form $\text{Al}(\text{ClO}_4)_3$: This dedoping behavior is spectrophotometrically demonstrated in Figure 3.

The fading of the Al and PCz films shown in Figure 2 was also observed when using PF_6^- and BF_4^- as the dopant instead of ClO_4^- . Figure 4 displays SEM images of the surface of the PCz films doped with ClO_4^- (a), PF_6^- (b), and BF_4^- (c). These green-colored films were prepared at 1.2 V ($Q = 60 \text{ mC cm}^{-2}$) in dichloromethane solutions containing 0.1 M TBAP (a), TBAPF_6 (b), and TBABF_4 (c), respectively. As is often the case with electropolymerized films, the film structure is strongly dependent on the dopant type, and the roughness of the PCz film is in the increasing order of $\text{ClO}_4^- > \text{PF}_6^- > \text{BF}_4^-$. Upon Al deposition (thickness = 15 nm) on these ClO_4^- , PF_6^- , and BF_4^- -doped films, the fading reaction occurred and was nearly completed in $t = \text{ca. } 2, 3, \text{ and } 4 \text{ h}$, respectively. These results suggest that a longer period of time is required for the complete fading of the PCz film with a smoother structure or less structural defects. This finding is consistent with the corrosion model described above and suggests that the reaction occurs at the structural defects at which PCz, Al, and water may coexist.

Though not shown here, a drastic color change to a nearly transparent pale yellow was observed upon contacting of the ClO_4^- -doped PCz film with an In layer. This fading reaction proceeded more rapidly than that for the PCz/Al system and was completed in $t = \text{ca. } 1 \text{ h}$. The difference in their reaction rates may be due to the difference in ϕ between Al ($\phi = 4.3 \text{ eV}$) and In ($\phi = 4.1 \text{ eV}$).¹⁴

3.3. Morphology of the PCz/Al Film along the Thickness. Part a in Figure 5 shows the TEM image of the cross section of the PCz/Al film, and part b in the figure is the TEM image to explain how the EDX analyses were conducted. The PCz film was prepared at 1.2 V ($Q = 28 \text{ mC cm}^{-2}$) in a dichloromethane solution containing 0.1 M TBAP, and then the Al film (8 nm in thickness) was deposited on it. The resultant PCz/Al film consists of bright and dark regions, the latter nanosized region being dispersed in the former background region. The EDX spectra taken at points 1 (bright region) and 2 (dark region) in image b are shown in parts c and d in Figure 5, respectively. The former spectrum exhibited signals corresponding to carbon (0.28 keV), but no chlorine signal (2.62 keV). This demonstrates that the bright region is composed of an undoped PCz. On

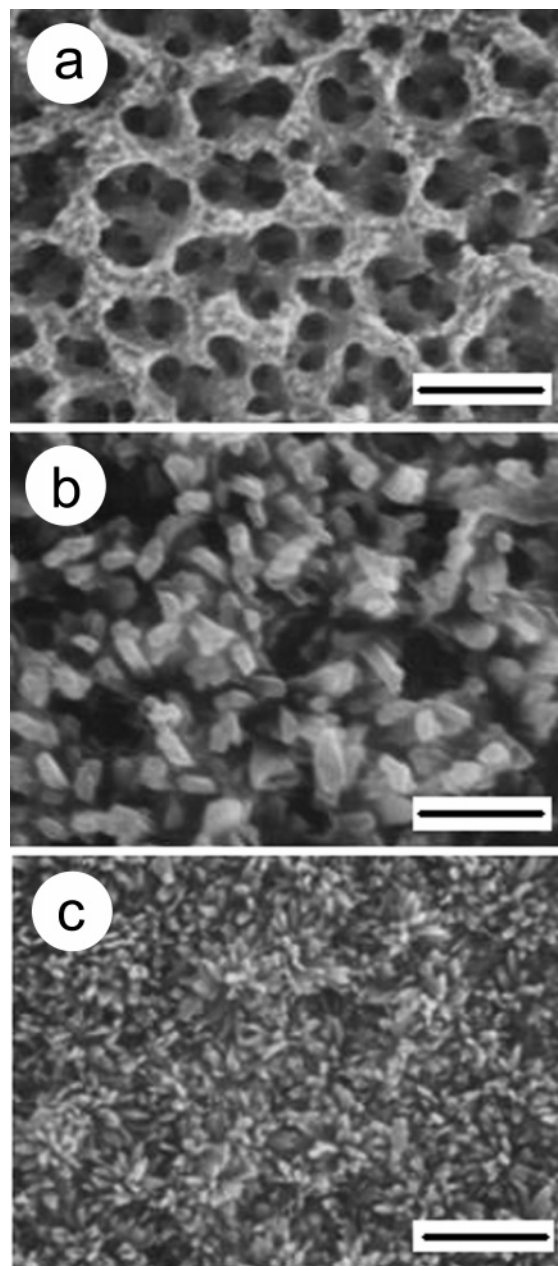


Figure 4. SEM image of the surface of the PCz films doped with ClO_4^- (a), PF_6^- (b), and BF_4^- (c). Scale bar: 2 μm .

the other hand, the latter spectrum has signals assignable to carbon (0.28 eV), oxygen (0.52 keV), aluminum (1.49 keV), and chlorine (2.62 keV), indicating that the dark region is the mixture of aluminum compounds and PCz. Parts e, f, and g show the depth profiles of Al, C, and O measured by EDX. The analyses were carried out along the line drawn in image b. The numerical values on the abscissa indicate the depth measured from the starting point (indicated by a circle in image b). The depth from 0.1 to 0.55 μm indicates the thickness of the PCz/Al film. The ranges of 0–0.1 μm and 0.55–0.65 μm correspond to the evaporated carbon layer and the ITO layer, respectively. In accordance with the above point analyses, Al and O were detected in the dark region, and their depth profiles (parts e and g) were in phase with each other, demonstrating that aluminum compounds, such as aluminum oxide/hydroxide and/or aluminum perchlorate, reside in the dark region. On the other hand, the bright region

(16) (a) Goddard, H. P. *Mater. Perform.* **1981**, *20*, 9–15. (b) Müller, B. *Farbe Lack.* **1997**, *103*, 24–29.

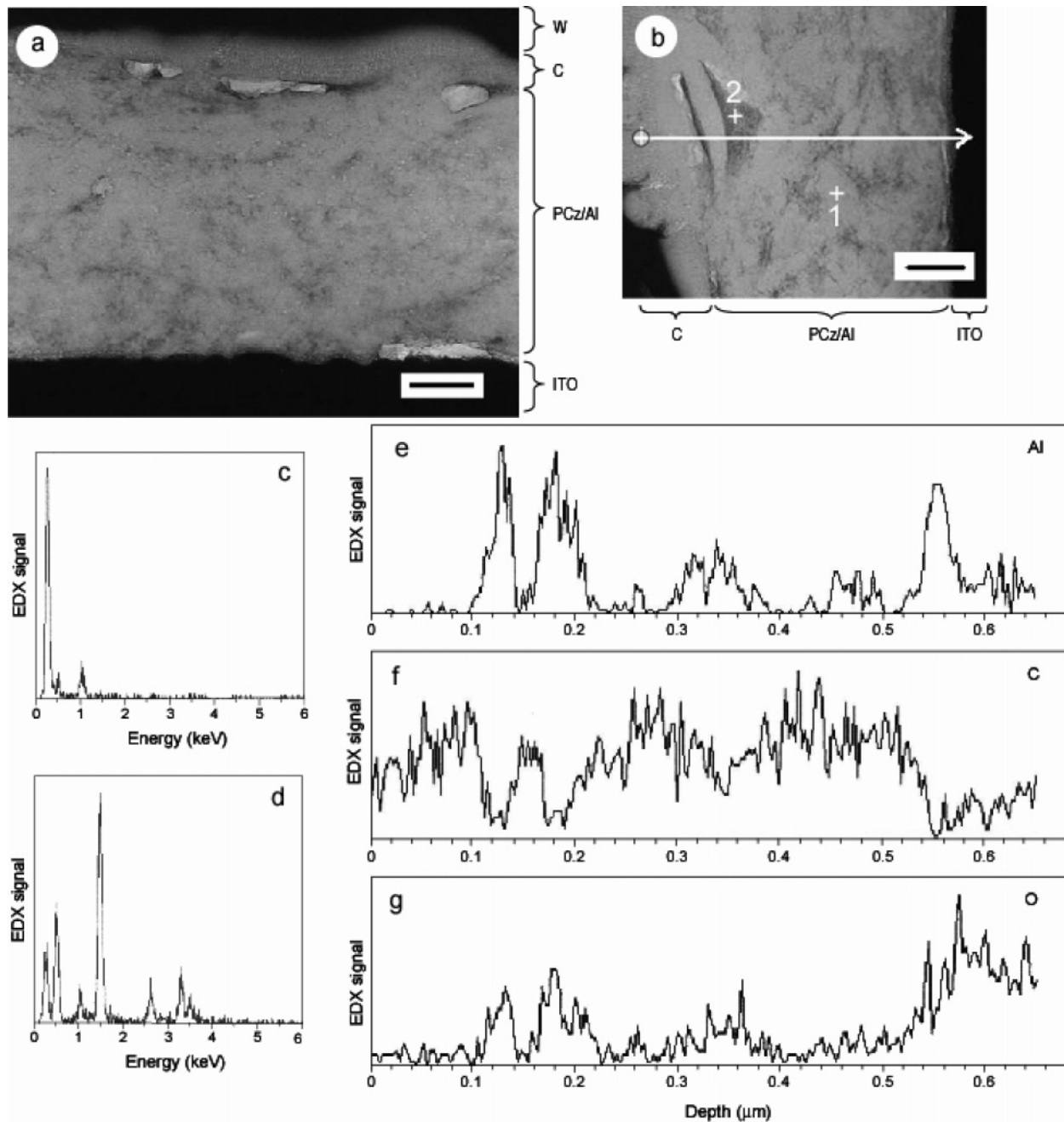


Figure 5. TEM image of the cross section of the PCz/Al hybrid film (a) and a similar cross-sectional view (b) to explain how the EDX point analyses (c, d) and the EDX line analyses on Al (e), C (f), and O (g) were conducted. Scale bars: 0.1 μm .

is rich in carbon and its depth profile (part f) was out of phase with those of Al and O. This indicates again that the bright region consists of undoped PCz.

Also, note that the dark region is distributed throughout the entire thickness range. As described in section 3.2, the evaporated Al layer on the PCz film was unaltered during its storage in a vacuum. This observation implies that the evaporated aluminum metal neither penetrates nor diffuses into the bulk of the PCz film. Therefore, the diffusion of Al^{3+} (an initially generated species as a result of electron exchange) may be required for the formation of the homogeneous distribution of the aluminum compounds. It may be that Al^{3+} is converted to aluminum oxide/hydroxide and aluminum perchlorate by the action of adsorbed water and ClO_4^- , respectively, during its diffusion into the PCz film.

To exclude the possibility of metal penetration and diffusion, TEM observations and EDX line analyses were also carried out for the PCz/Au film. As mentioned in section 3.2, no corrosion and dedoping reactions occurred in this sample, and accordingly, we can evaluate the possibility of metal penetration and diffusion during and after the evaporation, respectively. Part a in Figure 6 shows the TEM images of the cross section of the PCz/Au film and the results of the line analyses (depth profiles) on Au (part b), C (part c), and O (part d) measured by EDX. The PCz film was prepared in the same manner as that in Figure 5. The line is drawn in part a and the numerical values on the abscissa in parts b, c, and d indicate the depth measured from the cross point in part a; the ranges of 0–0.04 μm , 0.04–0.45 μm , and 0.45–0.63 μm correspond to the evaporated carbon layer, the PCz/

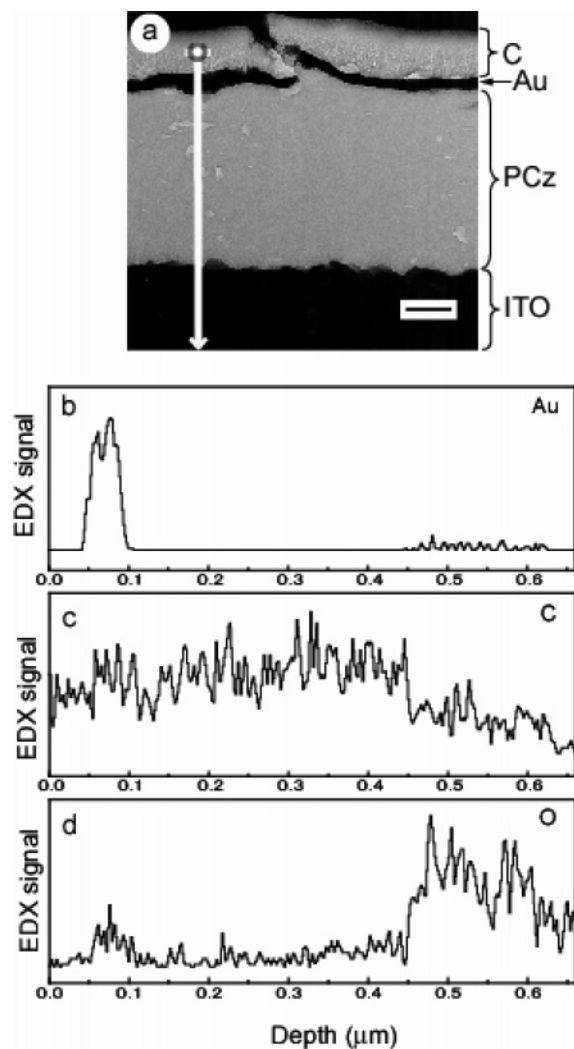


Figure 6. TEM image of the cross section of the PCz/Au film (a), and the depth profiles of Au (b), C (c), and O (d) measured by EDX. Scale bar: 0.1 μm.

Au film, and the ITO layer, respectively. As is evident from the depth profile in part b, the Au layer (dark region in part a) is pinned at the PCz film surface and did not diffuse into the PCz film bulk. Quite recently, we found that the layered structure of aluminum compounds and polymer material was formed depending on the kind of conducting polymer material. This provides feasibility to control morphology along the thickness by varying the kind of conducting polymer material, the details of which will be reported in a separate paper.

The XPS measurement was carried out on Al to understand its chemical states in the PCz/Al film. Though not shown here, the Al(2p) spectrum exhibited a signal at 74.8 eV. Based on the reported binding energies of Al₂O₃ (74.5 eV)¹⁷ and Al₂(SO₄)₃ (75.0 eV),¹⁸ this signal may arise from the superposition of those of Al₂O₃ and Al(ClO₄)₃. No metallic aluminum (71.6–73.0 eV)^{17b,19} was detected in the PCz/Al

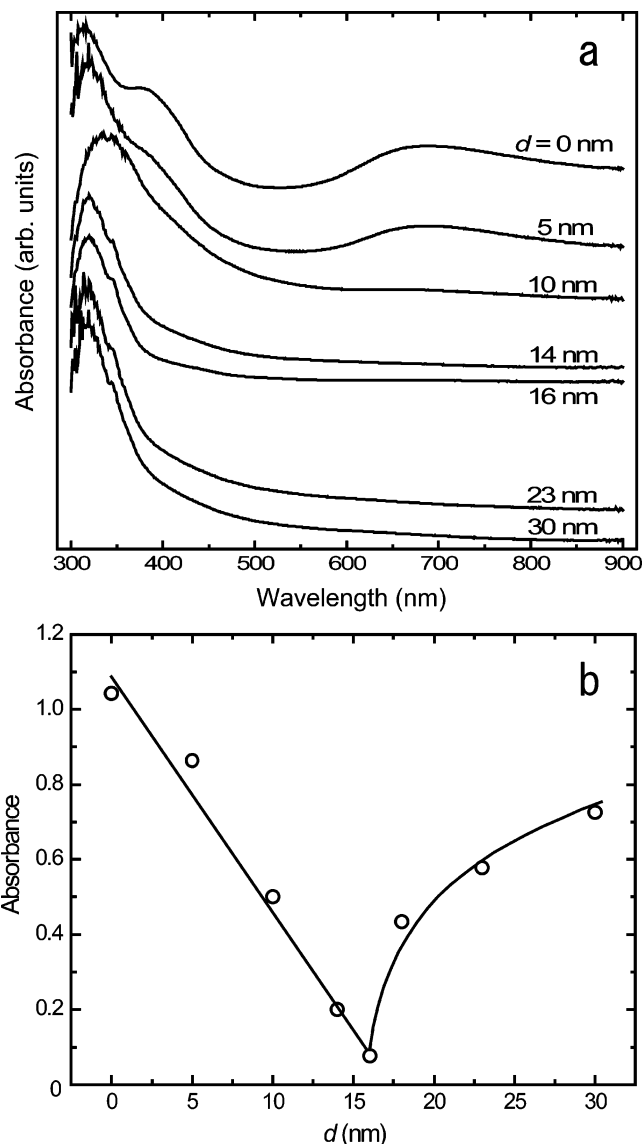


Figure 7. UV-vis absorption spectra of the PCz(960 nm)/Al films prepared by varying the thickness of the Al film, *d* (a), and the effect of *d* on the absorbance at 670 nm of the PCz/Al film (b).

film. The identification of the aluminum compounds in the PCz/Al film is of importance in connection with the mechanistic consideration, investigation to this end being in progress in the laboratory.

3.4. Stoichiometry for the Hybridization Reaction. It may be of fundamental and technological importance to know the maximum amount of the evaporated aluminum which completely reacts with the fixed amount of the PCz. Hence, the corrosion and dedoping reactions were investigated by varying the thickness of the Al film, *d* (this reaction couple will be hereinafter referred to as the hybridization reaction). Part a in Figure 7 shows the change in the UV-vis absorption spectrum of the PCz film with *d*, in which the ordinate is given in arbitrary units for the ease of appearance. The PCz film was prepared at 1.2 V ($Q = 60 \text{ mC cm}^{-2}$, 960 nm in thickness) in the dichloromethane/TBAP(0.1 M) system. The spectra were recorded after the hybridization reaction ceased. The absorption bands at 400 and 670 nm decreased with the increasing *d* and reached a minimum at *d* = 16 nm. When the *d* value increased beyond

(17) (a) Taylor, J. A. *J. Vac. Sci. Technol.* **1982**, *20*, 751–755. (b) Klein, J. C.; Hercules, D. M. *J. Catal.* **1983**, *82*, 424–441. (c) Strohmeier, B. R.; Hercules, D. M. *J. Phys. Chem.* **1984**, *88*, 4922–4929. (d) Strohmeier, B. R.; Leyden, D. E.; Field, R. S.; Hercules, D. M. *J. Catal.* **1985**, *94*, 514–530.

(18) Arata, K.; Hino, M. *Appl. Catal.* **1990**, *59*, 197–204.

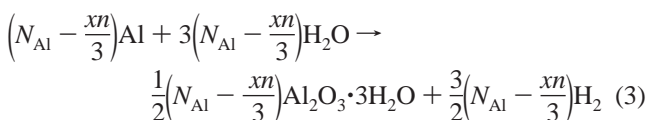
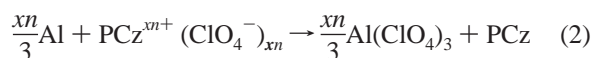
(19) Pashutski, A.; Folman, M. *Surf. Sci.* **1989**, *216*, 395–408.

16 nm, a part of the evaporated aluminum was not subject to the hybridization reaction. The unreacted aluminum increased the absorbance over the entire wavelength range. Therefore, the absorbance at 670 nm is a good measure for the determination of the extent to which the hybridization reaction proceeds. Part b in Figure 7 shows the change in the absorbance at 670 nm with d . The absorption minimum at $d = 16$ nm is clearly demonstrated and the d value corresponds to the maximum thickness of the Al film that completely reacts with the 960 nm thick PCz film.

The number of aluminum atoms in the 16 nm thick Al film per unit area, N_{Al} , was determined to be $9.64 \times 10^{16} \text{ cm}^{-2}$ using the density (2.70 g cm^{-3})²⁰ and the atomic weight (26.98 g mol^{-1}). The value of Q consists of the amounts of electricity passed during the electrochemical polymerization of carbazole and the doping of ClO_4^- in the generated PCz film. The former and the latter amounts are given by $2(n - 1)e$ and xne , respectively, where n , x , and e denote the number of carbazole units involved in the PCz film per unit area, the doping level of the PCz film, and elementary charge, respectively.

$$Q = 2(n - 1) + xne \quad (1)$$

This relationship allowed us to calculate the value of n , $1.5 \times 10^{17} \text{ cm}^{-2}$, and the number of ClO_4^- , $xn = 8.0 \times 10^{16} \text{ cm}^{-2}$, for the 960 nm thick PCz film using the value of x ($=0.54$) determined by the XPS measurements and the amount of Q ($=60 \text{ mC cm}^{-2}$). If we assume that the Al atoms are consumed by the dedoping and the corrosion reactions, the following relationships can be expected to hold:



Equation 2 shows the complete reduction of the ClO_4^- -doped PCz, $\text{PCz}^{xn+}(\text{ClO}_4^-)_{xn}$, by the action of Al to form $\text{Al}(\text{ClO}_4)_3$ and the undoped PCz. The rest of the evaporated Al is corroded to form $\text{Al}_2\text{O}_3 \cdot 3\text{H}_2\text{O}$ ^{15b,16} according to eq 3. These assumptions allowed us to estimate the fractions of Al atoms taking part in the dedoping reaction, 28%, and those in the corrosion reaction, 72%. This result in turn gives the mole ratio of the reaction products, $\text{Al}(\text{ClO}_4)_3:\text{Al}_2\text{O}_3 = 7:9$.

3.5. Electronic Properties of Al/PCz Films. As described in section 3.4, the hybridization reaction involves the dedoping of the PCz film. This implies that the electronic properties of the PCz film are perturbed by the reaction; hence, the electric conductivity and the work function measurements were carried out for the PCz/Al films. The electric conductivity (σ) was measured by the four-point probe method. The PCz and PCz/Al films strongly adhere to the ITO plate and could not be peeled off with an adhesive tape, so the test samples were prepared as follows. The PCz

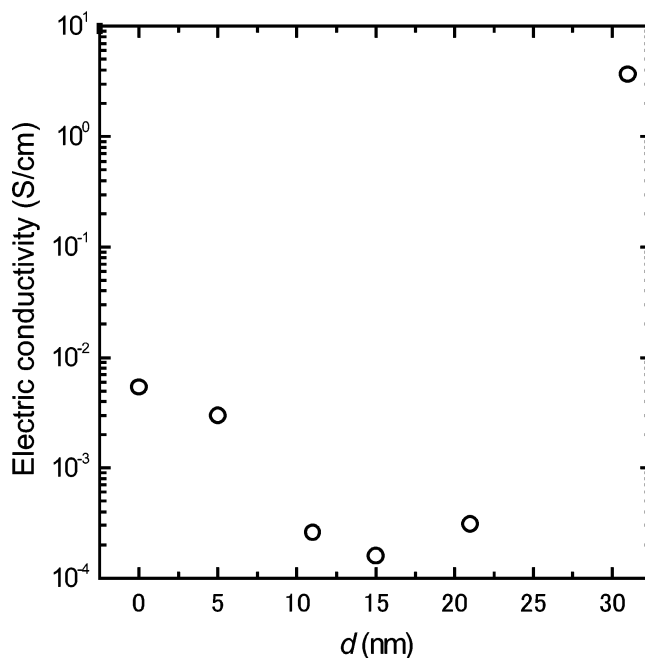


Figure 8. Dependence of electric conductivity (σ) of the PCz(960 nm)/Al film on the thickness of the evaporated Al film (d).

films were prepared in a manner similar to that in section 3.4 and dipped in a binder polymer solution consisting of polycarbonate (Teijin Chemicals Panlite K-1300Y, resistivity $\geq 1 \times 10^{15} \Omega\text{-cm}$), dichloromethane, and chloroform (1:8:8 in weight ratio). The samples were then pulled out of the solution and dried at $60 \text{ }^\circ\text{C}$ for 3 h. The resultant PCz films covered with the polycarbonate layer are easily stripped from the ITO plate. The PCz/Al hybrid films were prepared by evaporating Al onto the PCz film side of the free-standing polycarbonate-coated PCz films. Figure 8 shows the relationship between the σ value of the PCz/Al film and d . The σ value for the PCz single film (corresponding to $d = 0$ nm), $5.4 \times 10^{-3} \text{ S cm}^{-1}$, agrees well with the reported values,⁸ 10^{-4} to $10^{-3} \text{ S cm}^{-1}$. The value of σ decreases and, after passing through a minimum ($\sigma = 1.6 \times 10^{-4} \text{ S cm}^{-1}$) at $d = 15$ nm, increases with increasing d . The decline of σ to a minimum and its subsequent rise would be explained by the dedoping of the PCz film and the effect of the unreacted Al metal remaining on the film surface, respectively. This result supports the finding in section 3.4 that the 16 nm thick Al film stoichiometrically reacts with the 960 nm thick PCz film. Also note that the extent to which the value decreased by the hybridization is quite small. This is in contrast to the general findings that the electric conductivity of the conducting polymers decreases by several orders of magnitude upon their dedoping.^{1b} The noninsulating feature of the stoichiometric hybrid film, PCz(960 nm)/Al(16 nm), is noteworthy when coupled with its nearly transparent white color; its transmittance in the visible-light region is ca. 83% as shown in Figure 7 since transparent flexible organic electrodes²¹ have been required in large-area electronics such as photovoltaic devices, organic electroluminescent displays, liquid crystal displays, and electronic papers. We have demonstrated the possibility of using the hybrid film as an organic electrode; however, the still limited conductivity of the hybrid film with respect to the previously reported material (poly-

(20) Budavari, S.; O'Neil, M. J.; Smith, A.; Heckelman, P. E.; Kinneary, J. F. *The Merck Index*; Merck & Co., Inc.: Whitehouse Station, 1991; p 58.

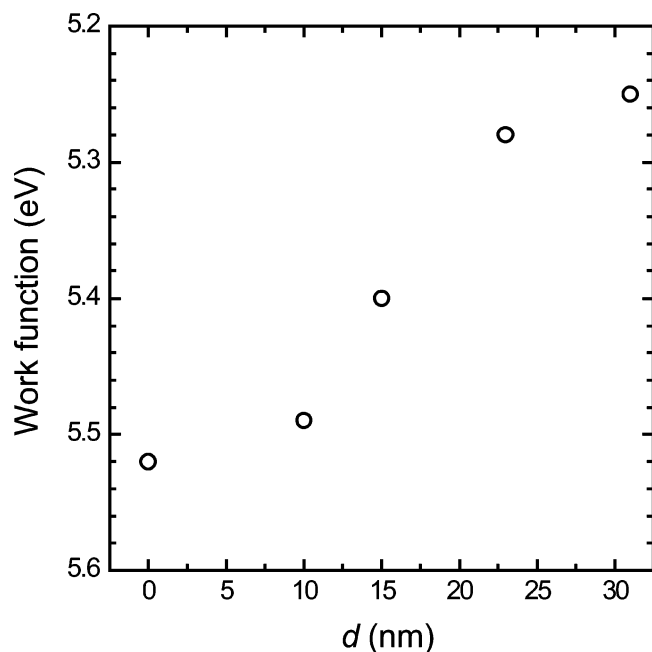


Figure 9. Dependence of work function (ϕ) of PCz(960 nm)/Al film on the thickness of the evaporated Al film (d).

(3,4-ethylenedioxythiophene) doped with poly(styrenesulfonate)^{21b-e}) should be improved. The reason for the slight decrease in σ is likely to be due to the action of the generated aluminum salt and/or aluminum oxide/hydroxide dispersed in the PCz film. However, the elucidation of the electric conduction mechanism for such a complex hybrid material would be far from simple and cannot be clarified at this time.

Figure 9 shows the work function (ϕ) of the PCz/Al film plotted vs d . The value of ϕ was calculated on the basis of the following relationship¹⁰

$$\phi = \phi_{\text{Au}} - \text{CPD} \quad (4)$$

where ϕ_{Au} shows the work function of the vacuum-evaporated Au film ($\phi_{\text{Au}} = 5.1$ eV).¹⁴ The measurements were carried out under ambient conditions of temperature and pressure. To check the measurement system, the ϕ values of a vacuum-evaporated Al film and the ITO plate were measured; the former and the latter values were 4.21 and 5.26 eV, respectively, being in good agreement with the reported values (4.28 eV¹⁴ for Al and 5.28 eV²² for the ITO). The PCz and PCz/Al hybrid films were prepared on the ITO in a manner similar to that in section 3.4. The value of ϕ for the single PCz film, 5.52 eV, decreased with the increasing d . Chowdhury et al.²³ measured the work function of the

PF₆⁻-doped poly(3-methylthiophene) films and showed that the ϕ value for the heavily doped film, 5.4 eV at a doping level of 0.24, decreased to 4.9 eV due to its dedoping. They explained this trend in terms of a change in the Fermi level expected for traditional inorganic semiconductors. Based on this report, the decrease in ϕ with d in the range of $0 < d \leq 15$ nm in Figure 9 may be again explained by the dedoping of the PCz film and the further decrease above $d = 15$ nm by the effect of the unreacted Al metal.

3.6. Electrochemical Properties of Al/PCz Films. Our previous study^{4c} revealed that the durability of the PPy film against electrochemical redox cycling was improved by the hybridization with Al or In and that the improvement was explained by assuming that the cross-linking²⁴ and/or over-oxidation²⁵ are blocked by the presence of the metal oxide intertwined between the polymer chains. Thus, the durability of the PCz/Al film was also examined in comparison with the PCz single film. Figure 10 shows the repetitive cyclic voltammograms of the PCz (a) and the PCz/Al films (b) measured in dichloromethane/TBAP(0.1 M). The PCz film was prepared at 1.2 V ($Q = 60$ mC cm⁻²) in a dichloromethane solution containing 0.1 M of TBAP, and then the Al film (15 nm in thickness) was deposited on it. The oxidation wave is assignable to the conversion of the noncharged benzenoid structure into the positively charged structure consisting of quinoid and benzenoid units containing ClO₄⁻ as a dopant, and the reduction wave corresponds to the conversion of the latter to the former structure.^{6a,c,d} Mengoli et al.^{6a} investigated the cyclic voltammetric behavior of a PCz film in acetonitrile containing TBAP and reported that an irreversible degradation occurred shortly afterward due to minor dissolution, swelling, and detachment of the film from the substrate electrode. In accordance with this report, the voltammograms of the PCz single film are unstable against the repeated redox cyclings (part a in Figure 10). However, the voltammograms of the PCz/Al film reached reproducible patterns after the fifth redox cycling (part b in Figure 10), indicating good durability against electrochemical redox cycling. Part c in Figure 10 shows the tenth redox cycles of the PCz single film (solid curve) and the PCz/Al film (dotted curve). The redox waves of the latter voltammogram are larger than those of the former voltammogram, also being the support for the action of aluminum oxide/hydroxide and/or salt on the retardation of the polymer degradation.

To understand the action of the aluminum compounds, FT-IR measurements were undertaken before and after the hybridization. Figure 11 shows the FT-IR spectra of the PCz single film (a) and the PCz/Al film (b). Their preparation conditions were the same as those of the films employed in the above cyclic voltammetry. The former spectrum is in excellent agreement in shape and positions of peaks with

(21) (a) Tracz, A.; Jeszka, J. K.; Sroczynska, A.; Kryszewski, M. Schrader, S.; Pfeiffer, K.; Ulański, J. *Adv. Mater. Opt. Electron.* **1996**, *6*, 330–334. (b) Martin, B. D.; Nikolov, N.; Pollack, K.; Sapirgin, A.; Shashidhar, R.; Zhang, F.; Heiney, P. *Synth. Met.* **2004**, *142*, 187–193. (c) Aernouts, T.; Vanlaeke, P.; Geens, W.; Poortmans, J.; Heremans, P.; Borghs, S.; Mertens, R.; Andriessen, R.; Leenders, L. *Thin Solid Films* **2004**, *451–452*, 22–25. (d) Winther-Jensen, B.; Krebs, F. C. *Sol. Energy Mater. Sol. Cells* **2006**, *90*, 123–132. (e) Admassie, S.; Zhang, F.; Manjo, A. G.; Svensson, M.; Andersson, M. R.; Inganäs, O. *Sol. Energy Mater. Sol. Cells* **2006**, *90*, 133–141. (22) (a) Nagatomo, T.; Shinohara, I.; Takeuchi, M.; Omoto, O. In *Technical Digest of the 1st International Photovoltaic Science and Engineering Conference*; Hamakawa, Y., Ed.; Kobe, 1984; p 755. (b) Tadayyon, S. M.; Grandin, H. M.; Griffiths, K.; Coatsworth, L. L.; Norton, P. R.; Aziz, H.; Popovic, Z. D. *Org. Electron.* **2004**, *5*, 199–205.

(23) Chowdhury, A.-N.; Harima, Y.; Kunugi, Y.; Yamashita, K. *Electrochim. Acta* **1996**, *41*, 1993–1997.

(24) (a) Carlier, V.; Skompska, M.; Herman, C. B. *J. Electroanal. Chem.* **1998**, *456*, 139–152. (b) Kvinge, L. H. M.; Havinga, E. E.; Donkers, J. J. T. M. *Synth. Met.* **1993**, *54*, 453–460.

(25) Masalles, C.; Llop, J.; Viñas, C.; Teixidor, F. *Adv. Mater.* **2002**, *14*, 826–829.

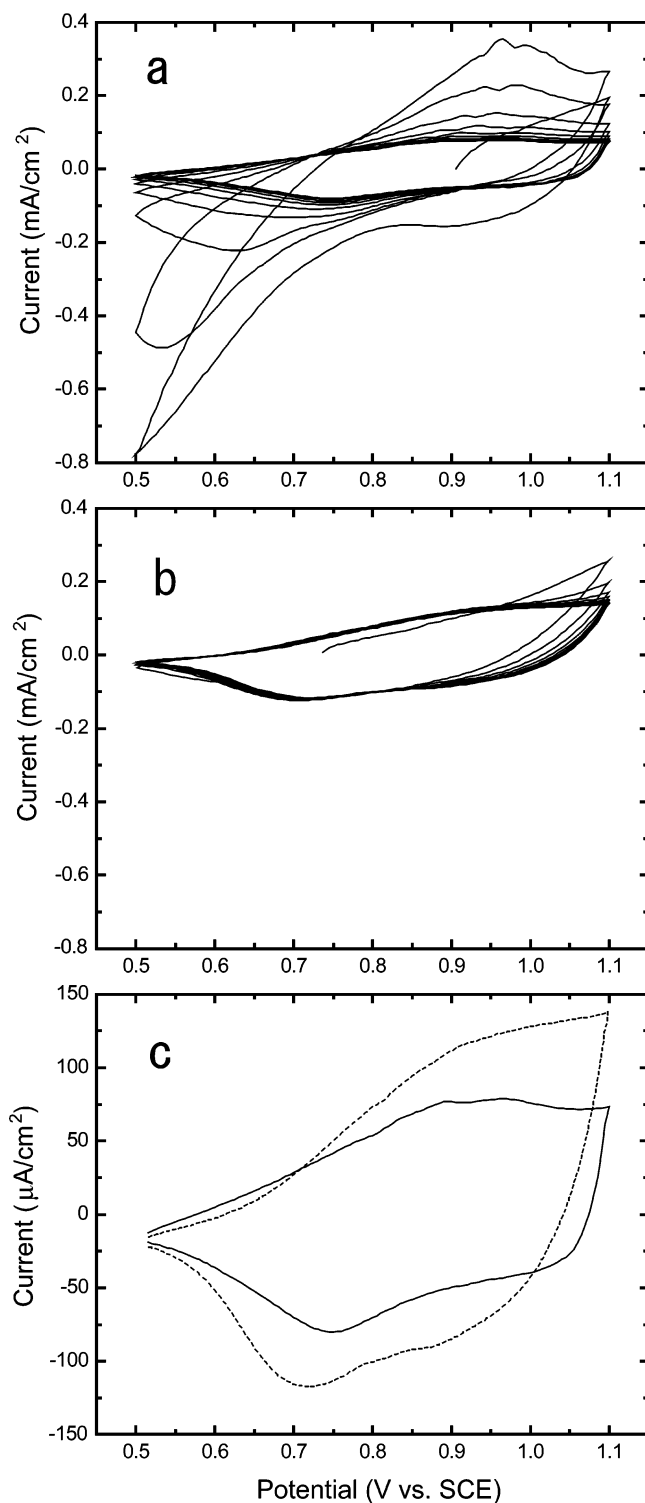


Figure 10. Cyclic voltammograms of the PCz single film (a) and the PCz/Al hybrid film (b) in dichloromethane/TBAP(0.1 M) for 10 repetitive potential sweeps between 0.5 and 1.1 V vs SCE. Part (c) shows the tenth redox cycle of the former (solid curve) and the latter films (dotted curve). Sweep rate: 20 mV/s.

that of the previously reported ClO₄⁻-doped PCz film.²⁶ The N–H stretching mode appeared at 3400 cm⁻¹. The spectrum of the PCz film showed a featureless decrease in absorption from 4000 to 1700 cm⁻¹, which is the tail of the near-IR absorption (~0.7 eV)²⁶ characteristic of the oxidized PCz. On the other hand, the absorption tail is depressed in

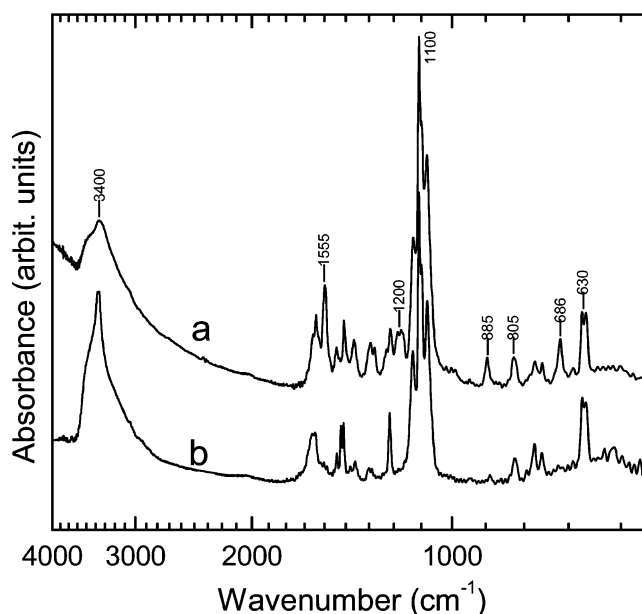


Figure 11. FT-IR spectra of the PCz single film (a) and the PCz/Al hybrid film (b) in KBr matrix.

spectrum b and the sharp signal due to N–H stretching was observed. These features are characteristic of the undoped PCz film,²⁷ indicating that the hybridization reaction is accompanied by the dedoping of the film. The signal seen at 1555 cm⁻¹ in spectrum a is a ring vibration band characteristic of the oxidized (doped) PCz²⁶ and disappears in the spectrum of the reduced (undoped) state.²⁷ The absence of this signal in spectrum b also indicates that the hybridization involves the dedoping of the film.

The band at ca. 1200 cm⁻¹ in spectrum a is an N–H in-plane bending mode,²⁸ which is normally observed in the spectra of both the oxidized and the reduced states.^{26,27} However, spectrum b does not have this band, implying that the bending mode is disturbed by the interaction between the N–H moiety and the aluminum compounds. Support for the presence of this interaction was furnished by the change in the signal at 686 cm⁻¹ by the hybridization reaction. The signal seen in spectrum a is assigned to the out-of-plane bending of N–H²⁹ and also disappeared after the hybridization reaction (spectrum b).

The different types of adjacent C–H out-of-plane wag vibrations were seen in spectrum a at 885 and 805 cm⁻¹, which are one lone C–H and two adjacent C–H, respectively.²⁹ This observation shows evidence for the presence of trisubstituted benzene ring and indicates that polymerization may proceed at the 3 and 6 positions.³⁰ After the hybridization reaction, the former signal at 885 cm⁻¹ was disturbed (spectrum b). This implies that the aluminum compounds interact with the carbazole ring at the 4 and 5 positions. On the other hand, the latter signal at 805 cm⁻¹ was also observed in spectrum b. Therefore, we can assume

(27) Wei, Z.; Xu, J.; Nie, G.; Du, Y.; Pu, S. *J. Electroanal. Chem.* **2006**, *589*, 112–119.

(28) Lee, S. Y.; Boo, B. H. *J. Phys. Chem.* **1996**, *100*, 15073–15078.

(29) Lao, W.; Xu, C.; Ji, S.; You, J.; Ou, Q. *Spectrochim. Acta Part A* **2000**, *56*, 2049–2060.

(30) (a) Saraç, A. S.; Sezer, E.; Ustamehmetoğlu, B. *Polym. Adv. Technol.* **1997**, *8*, 556–562. (b) Macit, H.; Sen, S.; Saçak, M. *J. Appl. Polym. Sci.* **2005**, *96*, 894–898.

(26) Hayashida, S.; Sukegawa, K. *Synth. Met.* **1990**, *35*, 253–261.

no chemical interaction at the 1, 2, 7, and 8 positions. The bands near 1100 and 630 cm^{-1} are due to incorporated ClO_4^- ions in the PCz.^{26,30a,31} The frequency and the intensity of these bands were little affected by the hybridization, and hence, the dopant ClO_4^- ions were not modified by the hybridization reaction.

The FT-IR measurements described above gave a clue to the improvement in the durability of the PCz film by the hybridization reaction. The results showed evidence for the chemical interaction of the aluminum compounds with the PCz units at the 4, 5, and 9 positions. The most likely explanation for the improvement resulting from the hybridization is that the interaction gives rise to the networks of the PCz chains with attached aluminum compounds, leading to the prevention of the PCz from dissolving in the electrolyte solution during the redox cyclings.

4. Conclusions

An anion-doped and green-colored PCz film was potentiostatically prepared (section 3.1) and its solid-state reaction with an evaporated aluminum film was investigated (section 3.2). The reaction produced a colorless hybrid film composed of undoped PCz and aluminum compounds (aluminum oxide/hydroxide and aluminum salt). Some control experiments and spectroscopic analyses revealed that the hybridization is based on the galvanic corrosion reaction and the dedoping reaction of the PCz film. The fractions of aluminum atoms participating in the former and the latter reactions were estimated as 72 and 28%, respectively, on the basis of the

stoichiometric considerations combined with the spectroscopic analyses (section 3.4). Electron micrographic observations coupled with microscopic analyses demonstrated the unique nanostructure of the hybrid film (section 3.3); the nanosized region of the aluminum compounds is almost homogeneously dispersed in the undoped PCz film. The stoichiometric hybrid film is characterized by its nearly transparent appearance (transmittance: ca. 83% in the visible-light region) and its noninsulating feature (electronic conductivity: $1.6 \times 10^{-4} \text{ S cm}^{-1}$) (section 3.5). These features suggest its feasibility for use as a transparent flexible organic electrode though the electric conductivity is still limited. Besides these spectroscopic and electronic modifications, hybridization also affected the electrochemical property of the PCz film: The improvement in the durability of the PCz film against the electrochemical redox cycling was obtained by hybridization (section 3.6). FT-IR measurements of the films before and after the hybridization reaction suggested chemical interaction between the PCz backbone and the aluminum compounds which may prevent dissolution of the PCz during the electrochemical redox cyclings, resulting in the improvement in its durability.

We are beginning to extend this finding to the fabrication of PCz/Zn and PCz/Ti hybrid systems, the details of which will be reported elsewhere.

Acknowledgment. This research was partially supported by grants from Tokyo Ohka Foundation for the Promotion of Science and Technology and from the Ministry of Education, Science, Sports and Culture, Grant-in-Aid for Exploratory Research, No. 15655079.

(31) Ghita, M.; Arrigan, D. W. M. *Electroanalysis* **2004**, *16*, 979–987.